JSE Journal of Systematics and Evolution

doi: 10.1111/jse.12545

Research Article

Genetic diversity of *Cedrela fissilis* (Meliaceae) in the Brazilian Atlantic Forest reveals a complex phylogeographic history driven by Quaternary climatic fluctuations

Érica Mangaravite[1,2,3]*, Thamyres C. da Silveira[1], Alexander Huamán-Mera[1,4], Luiz O. deOliveira[1], Alexandra N. Muellner-Riehl[5,6], and Jan Schnitzler[3,5,6]*

[1]Laboratory for Molecular Biology and Phylogeography, Biochemistry Department, Federal University of Viçosa, Viçosa, Minas Gerais State, Brazil

[2]Department of Biomedicine, Health Science Center, Centro Universitário Unifaminas, Av. Cristiano Ferreira Varella, 655, Bairro Universitário, Muriaé, Minas Gerais State, Brazil

[3]Senckenberg Biodiversity and Climate Research Centre (SBiK-F), Frankfurt am Main, Germany

[4]Faculty of Forestry and Environmental Engineering, National University of Jaen, 250 Cuzco, Avenue, Jaen, Peru

[5]Department of Molecular Evolution and Plant Systematics & Herbarium (LZ), Institute of Biology, Leipzig University, Leipzig, Germany

[6]German Centre for Integrative Biodiversity Research (iDiv) Halle-Jena-Leipzig, Leipzig, Germany

*Authors for correspondence. Érica Mangaravite. E-mail: erica.mangaravite@gmail.com; Jan Schnitzler. E-mail: jan.schnitzler@uni-leipzig.de

Received 28 May 2019; Accepted 13 September 2019; Article first published online 7 October 2019

Abstract Quaternary climatic fluctuations have shaped the geographic distribution of lineages, potentially affecting the demography, genetic structure, and patterns of genetic diversity of extant species. Different phylogeographic scenarios have been proposed for plants in neotropical cloud forests during the Last Glacial Maximum based on paleoecological data: the dry refugia hypothesis (DRH) and the moist forest hypothesis. We specifically focus on the Brazilian Atlantic Forest (BAF) range of *Cedrela fissilis* (Meliaceae), sampling 410 specimens from 50 localities. Our study combines analyses of the genetic diversity, phylogeographic patterns, and past geographic distributions with a particular focus on highland populations. We identified 283 alleles across the 11 microsatellite loci, ranging from 18 to 33 alleles per locus, distributed across five genetic groups. Most populations of *C. fissilis* from the BAF exhibited a diffuse genetic structure, reflected in low pairwise F_{ST} values, which could be the consequence of high gene flow. In addition, the plastid data showed a connection between the western, southern, and eastern populations in the North-East of Brazil, but no association between genetic data and elevation was observed. Habitat suitability projections over the past 140 000 years showed less fragmentation relative to the present, indicating a higher connectivity and gene flow. Our results provide support for both the moist forest as well as the DRH, suggesting that most likely, a mixture of these processes has acted through space and time.

Key words: climate change, genetic diversity, habitat suitability, microsatellite, mountain, phylogeography.

1 Introduction

Mountain regions around the world are often exceptionally rich in biodiversity and endemism (Kier et al., 2009; Muellner-Riehl, 2019). In South America, the most important orographic features of the Atlantic coast are the mountains of the Serra do Mar and the Serra da Mantiqueira (Almeida & Carneiro, 1998), which have a strong influence on the climatic conditions in the South and Southeast of Brazil. Previous studies reported floristic similarities between these highlands (Bertoncello et al., 2011; Meireles & Shepherd, 2015), high tree species richness (Pompeu et al., 2014), and a high proportion of endemic species (Meireles et al., 2014). The mountains harbor part of the Brazilian Atlantic Forest (BAF) (Oliveira-Filho & Fontes, 2000), one of the 36 currently recognized global biodiversity hotspots with an exceptionally high number of endemic species (about 8000 are vascular plants species and almost 600 are vertebrate species, Myers et al., 2000) and a high level of habitat loss (Myers et al., 2000; Conservation International, 2018). Today, only about 11.4%–16% of the natural vegetation remains (Tabarelli et al., 2005; Ribeiro et al., 2009).

Climatic conditions shape the geographic distribution of species at medium to large spatial scales through time (e.g., latitudinal gradient of species richness, Mannion et al., 2014), with climatic changes potentially affecting their genetic diversity (Stewart et al., 2010; Homburg et al., 2013; Ramírez-Barahona &

This is an open access article under the terms of the Creative Commons Attribution NonCommercial License, which permits use, distribution and reproduction in any medium, provided the original work is properly cited and is not used for commercial purposes.

© 2019 The Authors. *Journal of Systematics and Evolution* published by John Wiley & Sons Australia, Ltd on behalf of Institute of Botany, Chinese Academy of Sciences

Eguiarte, 2013; Muellner-Riehl, 2019). Over time, climatic fluctuations can lead to a decline in genetic diversity and ultimately species extinction, or to divergence within species and, potentially, speciation (Hewitt, 2000). The Last Glacial Maximum (LGM, about 28 000 to 24 000 years ago; Hughes & Gibbard, 2015) was one of the largest manifestations of natural climate fluctuations that remains relatively well preserved in the geological record (Mix et al., 2001; Hughes & Gibbard, 2015). During the LGM, global climates were dramatically different from earlier times and from the climate of today (Mix et al., 2001), probably best depicted by the large extent of terrestrial glaciers. Although not representing a typical scenario during the Quaternary climate fluctuations, the LGM may likely have had a major impact on the geographic distribution and/or genetic diversity of species (Silva et al., 2012; Ramírez-Barahona & Eguiarte, 2013).

In South America, early studies suggested that cold and dry conditions in the Amazon region during the LGM would have led to forest fragments that served as refugia isolated by open non-forest vegetation (Haffer, 1969; Hammen & Hooghiemstra, 2000). In the south of the BAF, palynological data show that grasslands dominated the landscape during the LGM where forest ecosystems exist today, indicating a colder and drier climate (Behling, 2002). In addition, Carnaval & Moritz (2008) used palaeoclimatic models and predicted historical forest refugia within the BAF. They found that climatically more stable areas matched the current centers of endemism in five vertebrate species. Furthermore, studies on frog (Carnaval et al., 2009) and bird species (Amaral et al., 2013) suggested a dry refuge area in the BAF that could explain the high present-day biodiversity of this area. Contrary to these studies, some pollen data did not indicate a replacement of forest by grassland vegetation in Amazonia, suggesting that forest cover may have remained stable and not fragmented (Colinvaux et al., 2000; Rull, 2008). In addition, Leite et al. (2016) modeled an expansion of suitable climatic conditions onto the emerged continental shelf during the LGM for five species of small mammals, and suggested that forest refugia played only a minor role, if any, in this region during glacial periods. Also, a study on toads endemic to the BAF suggested the persistence of forested habitats in the south (Thomé et al., 2010) instead of a colonization from northern refugia after the LGM (Carnaval & Moritz, 2008).

Ramírez-Barahona & Eguiarte (2013) reviewed paleoecological records from the Neotropics and proposed two phylogeographic scenarios for cloud forests during the LGM: the dry refugia hypothesis (DRH) and the moist forest hypothesis (MFH). Under the DRH, geographic ranges would have contracted and become fragmented during the cooling phases, resulting in a loss of genetic diversity. Subsequent recolonization of uninhabited areas from small effective population sizes would cause a marked genetic structure. In addition, populations would show genetic differentiation, if they stemmed from different refugial lineages (Ramírez-Barahona & Eguiarte, 2013). In contrast, under the MFH, populations would move downslope to mid or low elevations during cooling phases, while increasing their connectivity. Afterward, during a warming phase, they would move upslope again and experience range fragmentation and little or no demographic expansion. The main consequence of this would be the increase in genetic diversity resulting from spatial heterogeneity and diffuse genetic structuring of populations (see Ramírez-Barahona & Eguiarte (2013) for more details). It should be noted, however, that these scenarios are based on the assumption that the mountain area size generally decreases with elevation (see their figure 2), but because of the heterogeneous topography of mountains, this is not always the case (Elsen & Tingley, 2015). More specifically, Elsen & Tingley (2015; their figure 1) showed that some mountains will have larger areas available at higher elevations, allowing for the possibility of population expansion (and connection) while moving upslope. Given that the mountains of both the Serra do Mar and the Serra da Mantiqueira are hourglass-shaped (sensu hypsographic classification of Elsen & Tingley, 2015), one might expect no general clear-cut genetic pattern, as described by the MFH across different elevational zones in this region. In addition, given the uncertainty concerning the increased aridity during times of lower temperature, it remains unsubstantiated whether cloud forests were contracted into forest refugia during the LGM or not (Ramírez-Barahona & Eguiarte, 2013). In the BAF's mountains, paleoecological and phylogeographic studies have shown agreement with the DRH (Behling, 2002), while others have not accepted the DRH (Thomé et al., 2010; Amaro et al., 2012).

Here, we evaluate the DRH and MFH hypotheses for the Brazilian Atlantic cloud forest using the neotropical tree species *Cedrela fissilis* Vell. (Meliaceae). Commonly called "cedro branco" or "cedro rosa" (Carvalho, 1994), *C. fissilis* is a deciduous tree that belongs to a genus with 19 hardwood species (Pennington & Muellner, 2010; Koecke et al., 2015; Huamán-Mera et al., unpublished data) and is widely distributed in seasonal forests and adjacent ecotones as well as gallery forests (Pennington et al., 1981; Carvalho, 1994; Pennington & Muellner, 2010). Garcia et al. (2011) explored phylogenetic relationships and the phylogeography of *C. fissilis* in Brazil and the eastern part of Bolivia. They found that the species consists of two distinct genealogical lineages: one centered in the Chiquitano range and the other one in the Atlantic range, separated by the Cerrado (Brazillian savanna). These patterns were confirmed using 10 microsatellite markers by Mangaravite et al. (2016). In the Atlantic range, populations occur from 20 m to more than 1600 m above sea level (Mangaravite et al., 2016). We specifically focus on the Atlantic range of *C. fissilis* with a substantially extended sampling and combine analyses of the genetic diversity, phylogeographic patterns, and past geographic distributions to evaluate the DRH and MFH hypotheses.

2 Material and Methods

2.1 Sampling strategy

We evaluated 410 specimens from 50 localities of *Cedrela fissilis* throughout the Atlantic range (Fig. 1). For the population genetic analysis, we genotyped 344 specimens from 21 populations, while we investigated 148 specimens from all 50 localities for the phylogeographic analysis, comprising both new collections and published data (Garcia et al., 2011; Mangaravite et al., 2016; Huamán-Mera et al., unpublished data). The population codes, localities, coordinates, number of specimens, and the references are shown in Table 1 and Table S1. The populations MDP, PEU, VNI, CAP, PSB, PSO, and PNI occur in elevations higher than 600 m a.s.l., hereafter referred to as highland populations (Fig. S1).

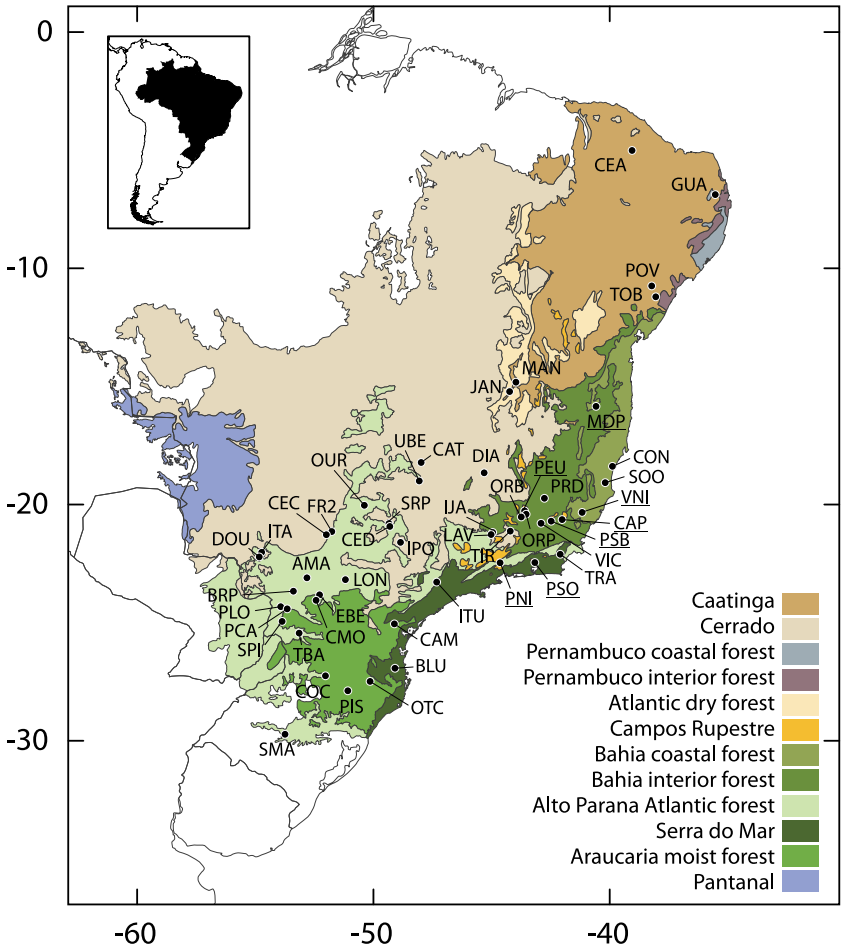


Fig. 1. Localities of sampled populations of *Cedrela fissilis* in eastern South America. The background map shows the terrestrial ecoregions within the study area (Olson et al., 2001; refer to Table S1 for population codes).

2.2 Species distribution modeling

Georeferenced occurrence localities of *C. fissilis* were compiled from field records and published data (Garcia et al., 2011; Mangaravite et al., 2016; Huamán-Mera et al., unpublished data). In total, we used 50 occurrences to model habitat suitability. To alleviate the impact of spatial autocorrelation, we only included records with a minimum pairwise distance of 10 km. The models were built using the maximum entropy algorithm as implemented in MAXENT (Phillips et al., 2006). In particular, we used a 10-fold cross validation approach with 80% of the occurrences for training and 20% for testing. To assess model performance, we used the area under the receiver operating characteristic (ROC) curve (AUC; Hanley & McNeil, 1982). The AUC determines the model's predictive ability compared to a random prediction. In addition, models were validated by assessing the sensitivity, specificity, and accuracy values averaged across the replicates. To estimate habitat suitability, we used bioclimatic variables from WorldClim (Hijmans et al., 2005) at 2.5 arcmin resolution as explanatory variables. From the 19 bioclimatic variables, we selected those with a Pearson correlation of less than 0.71 (Table S2) and as well as a high contribution and permutation importance in the models (Tables S3 and S4). We retained a subset of seven predictors: mean diurnal range (bio02), temperature seasonality (bio04), max temperature of warmest month (bio05), mean temperature of wettest quarter (bio08), precipitation of wettest quarter (bio16), precipitation of warmest quarter (bio18), and precipitation of coldest quarter (bio19).

For modeling, we used the *group discrimination* technique, which requires both presence and absence data (background) and has been shown to be more reliable than the *profile* technique (Mateo et al., 2010), which requires presence-only data. Mateo et al. (2010) showed that "target-group absences," instead of the use of random pseudo-absences, is more appropriate. Thus, instead of random, we calculated target-group absences using the *three-step* (TS) selection procedure as described in Iturbide et al. (2015). Also, we generated twice the number of presences as pseudo-absences for improving model reliability. The first step defines the environmentally unsuitable areas using a presence-only profiling algorithm; the second calculates different maximum distance thresholds to each presence location; and the last step selects the optimum background extent and the corresponding fitted model from all possible pseudo-absence configurations generated in step 2 (for more details see Iturbide et al., 2015). In addition, we included a 10 km of buffer around the collection localities to

Table 1 Populations of *Cedrela fissilis* and genetic diversity across 11 microsatellite loci

Locality (population code)	*n*	A_{priv}	A_{priv}/n	*A/locus*	H_E	H_O	*F*	Reference
Tobias Barreto and Poço Verde, SE (SER)	10	0	0	6.09	0.70	0.61	0.13	Mangaravite et al. (2016)
Januária, MG (JAN)	9	1	0.11	6.20	0.82	0.77	0.09	Mangaravite et al. (2016)
Mata do Passarinho, Bandeira, MG (MDP)	8‡							Huamán-Mera et al. (unpublished data)
Uberlândia, MG (UBE)	19	7	0.37	11.64	0.86	0.75	0.14	Huamán-Mera et al. (unpublished data)
Diamantina, MG (DIA)	13	3	0.23	10.18	0.86	0.73	0.16	Mangaravite et al. (2016)
Conceição da Barra, ES (CON)	3‡							Present study
Sooretama, ES (SOO)	7‡							Present study
Rio Doce State Park, MG (PRD)	3‡							Huamán-Mera et al. (unpublished data)
Uaimií State Park, MG (PEU)	17	4	0.24	11.18	0.84	0.75	0.11	Huamán-Mera et al. (unpublished data)
Venda Nova do Imigrande, ES (VNI)	37	4	0.11	12.64	0.80	0.68	0.15	Present study
Caparaó Nacional Park, MG, (CAP)	35	8	0.23	13.55	0.82	0.73	0.11	Mangaravite et al. (2016)
Serra do Brigadeiro State Park, MG (PSB)	10	2	0.20	8.64	0.83	0.64	0.24	Huamán-Mera et al. (unpublished data)
Aguapei river mouth, SP (FR2)	5‡							Huamán-Mera et al. (unpublished data)
Itaporã, MS (ITA)	9	3	0.33	7.55	0.83	0.72	0.14	Mangaravite et al. (2016)
Serra dos Órgãos Nacional Park, RJ (PSO)	25	9	0.36	11.91	0.87	0.74	0.16	Present study
Itatiaia Nacional Park, RJ (PNI)	61	8	0.13	16.27	0.86	0.71	0.17	Present study
Três Barras do Paraná, PR (TBA)	13	3	0.23	9.64	0.88	0.79	0.10	Mangaravite et al. (2016)
Palotina, PR (PLO)	28	6	0.21	13.27	0.86	0.72	0.16	Mangaravite et al. (2016)
Campinhos, PR (CAM)	7‡							Mangaravite et al. (2016)
Blumenau, SC (BLU)	18	3	0.17	11.09	0.82	0.72	0.11	Mangaravite et al. (2016)
Santa Maria, MS (SMA)	7‡							Mangaravite et al. (2016)
Overall sum	304 §	61 §	0.20					
Overall mean	21.71 §	4.35 §		10.70 §	0.83 §	0.72 §	0.14 §	

Note: ‡populations with $n < 9$; §values which do not include data from populations with $n < 9$; *n*, number of samples evaluated; A_{priv}, number of private alleles; *A/locus*, mean number of alleles per locus; H_E, expected heterozygosity; H_O, observed heterozygosity; *F*, inbreeding coefficient.

avoid grid cells with both presence and pseudo-absence data (Mateo et al., 2010; Iturbide et al., 2015).

The present-day model predictions were projected onto three past climatic layers: the Middle Holocene (MidHol) period about 6000 years ago, the LGM period about 28 000–24 000 years ago, and the last interglacial (LIG) period 120 000 to 140 000 years ago. For the MidHol and LGM, we created an average of three circulation models: CCSM4 (Gent & Danabasoglu, 2011), MIROC-ESM (Watanabe et al., 2011), and the MPI-ESM-P (Earth System Model of Max Planck Institute for Meteorology, Hamburg, Germany; Giorgetta et al., 2013). For the LIG, we employed the data from Otto-Bliesner et al. (2006). We calculated range fragmentation of *C. fissilis* for all four predictions in R (v.3.3.1, R Core Team 2016), using the package "SDMTools" (VanDerWal et al., 2014). First, we converted the habitat suitability scores (ranging from 0 to 1) into binary data according to different cutoffs (0.4, 0.5, 0.6, 0.7, and 0.8). At each level, we then measured the ratio between the patch perimeter (m) and the area (m^2) using the "PatchStat" function.

2.3 DNA extraction, microsatellite genotyping, and gene sequencing

Leaf samples were dried using silica gel and kept at room temperature until the DNA was extracted. Total genomic DNA was extracted according to Cota-Sánchez et al. (2006) with modifications (Riahi et al., 2010). Genotyping was carried out using 11 microsatellite loci: 8 markers (Ced2, Ced18, Ced41, Ced44, Ced54, Ced65, Ced95, and Ced1; Table 2) developed by Hernández et al. (2008) for *Cedrela odorata*, and three markers (CF26 and CF66) developed by Gandara et al. (2014) for *C. fissilis* (Table 2). Primer pair CF66 amplified two loci—CF66A and CF66B, respectively (Gandara et al., 2014); distinct ranges of allele sizes (113–167 bp for CF66A; 199–253 bp for CF66B) allowed us to clearly differentiate the genotypes of each of the two loci (Table 2). The polymerase chain reaction (PCR) was performed in two multiplexes—when we amplified more than one marker in the same PCR, M1 (Ced54-Ced41) and M2 (Ced2-Ced65), then two other primers were amplified separately (Ced95 and Ced131) and combined with the M1 and to M2, respectively, to be genotyped together to reduce costs. Also, two primers were amplified separately, but combined later for

Table 2 Description of 11 microsatellite loci

Locus	Primer sequence (5′-3′)	Array	Fluorescence	N_A	Allele size (bp)	Missing data	Null allele mean frequency	Reference
Ced2	F: TTTGCTTTGAGAAACCTTGT R: AACTTTCGAATTGGTTAAGG	$(GA)_{20}$	6-FAM	22	131–241	6.4%	0.0365	Hernández et al. (2008)
Ced18	F: CAAAGACCAAGATTTGATGC R: ACTATGGGTGGCACAACTAC	$(GA)_{23}$	HEX	24	115–161	10.5%	0.0349	Hernández et al. (2008)
Ced41	F: TCATTCTTGGATCCTGCTAT R: GTGGGAAAGATTGTGAAGAA	$(TC)_{18}$	HEX	28	68–186	4.7%	−0.0140	Hernández et al. (2008)
Ced44	F: ACTCCATTAACTGCCATGAA R: ATTTTCATTCCCTTTTAGCC	$(TG)_{14}(AG)_{17}$	6-FAM	33	154–238	14.2%	−0.0098	Hernández et al. (2008)
Ced54	F: GATCTCACCCACTTGAAAAA R: GCTCATATTTGAGAGGCATT	$(GA)_{15}(AG)_6G(GA)_5$	6-FAM	18	100–218	12.8%	0.0095	Hernández et al. (2008)
Ced65	F: GAGTGAGAAGAAGAATCGTGATAGC R: GAGGTTCGATCAGGTCTTGG	$(GA)_7(CA)_{14}$	HEX	20	121–199	16.0%	0.1655	Hernández et al. (2008)
Ced95	F: ATTTTCATTCCCTTTTAGCC R: TTATCATCTCCCTCACTCCA	$(CT)_{17}(AC)_{13}$	NED	31	115–253	24.7%	0.0160	Hernández et al. (2008)
Ced131	F: CTCGTAATAATCCCATTCCA R: GGAGATATTTTTGGGGTTTT	$(CT)_{16}$	NED	29	66–172	15.4%	0.1002	Hernández et al. (2008)
CF26	F: CCAAATTCCAGAGGAGAG R: GTTCTGCTTCATCGAAGG	$(GA)_9$	6-FAM	25	119–191	9.90%	0.1823	Gandara et al. (2014)
CF66A	F: CAGCAGTTCTGAAACAGTAA R: ATTCAGCAACTTGAGAGC	$(GA)_{19}$	6-FAM	28	113–167	11.9%	0.0089	Gandara et al. (2014)
CF66B	F: CAGCAGTTCTGAAACAGTAA R: ATTCAGCAACTTGAGAGC	$(GA)_{19}$	6-FAM	25	191–253	15.1%	0.0974	Gandara et al. (2014)

Note: N_A, number of alleles per locus; bp, basepairs.

genotyping—pseudo-multiplex M3 (Ced18-CF26). Finally, the last markers (Ced44 and CF66) had amplification and genotyping carried out separately. We used 12 μL volumes with 10 ng of DNA, 1× buffer (0.01 mol/L Tris-HCl, pH 8.4, 0.05 mol/L KCl, and 1% Triton X-100), 0.2 μmol/L of each primer (forward and reverse), 2.5 mmol/L of $MgCl_2$, 0.25 mg/mL of bovine serum albumin (BSA) (Invitrogen, São Paulo, Brazil), 0.2 mmol/L of dNTPs, and 0.5 U of Taq DNA polymerase (Phoneutria Biotecnologia, Belo Horizonte, Brazil). The amplifications were carried out on a Vapo Protect Eppendorf Thermal Cycler (Eppendorf; São Paulo, Brazil). In case of difficult amplification (as happened with primer Ced95), we conducted the PCR with 1× of the special buffer IVB (Phoneutria Biotecnologia, Belo Horizonte, Brazil). The amplification program (Gandara, 2009) consisted of a preheating step of 96 °C for 2 min, 30 cycles of 94 °C for 1 min, 55 °C for 1 min, and 72 °C for 1 min; at the end of the 30 cycles, there was an extension step of 72 °C for 7 min. Each forward primer was labeled with either 6-FAM, HEX (MWG-Biotech, Ebersberg, Germany), or NED (Applied Biosystems, São Paulo, Brazil) fluorescence (Table 2). Some of the fragments were separated on a 96-capillary sequencer ABI PRISM 3130 × 1 DNA Analyzer (Applied Biosystems, São Paulo, Brazil), and PCR products were sized relative to a molecular size marker (ROX 500—Applied Biosystems, São Paulo, Brazil). Part of the samples were genotyped by Macrogen Inc., South Korea (www.macrogen.com/), and the PCR products were sized relative to a molecular size marker (ROX 400). The fragments were scored using GeneMapper version 4.0 (Applied Biosystems, São Paulo, Brazil). For the 11 loci, the average percentage of missing data was 12.87% (ranging from 4.70%, for Ced41, to 24.7%, for Ced95).

The *trnT-trnL* spacer from the chloroplast genome was amplified using standard PCR protocols (Muellner et al., 2009; Oliveira et al., 2010). The spacer was amplified in two independent reactions. The first reaction was performed using the primers "a" and "b", which amplify the intergenic spacer between *trnT* (UGU) and the 5′ exon of *trnL* (UAA) (Taberlet et al., 1991). The second reaction was performed with primers "c" and "d" and amplified the intron of *trnL* (UAA) (Taberlet et al., 1991). The PCRs were carried out with 25 μL of final volume, with about 100 ng of DNA, 1× of the special buffer IVB (Phoneutria Biotecnologia, Belo Horizonte, Brazil), 0.5 μmol/L of each primer (forward and reverse), 2 mmol/L of $MgCl_2$, 17.5 μg/mL of BSA (Invitrogen, São Paulo, Brazil), 0.2 mmol/L of dNTPs, and 1.25 U of GoTaq DNA Polymerase (Promega, Belo Horizonte, Brazil). Amplifications were carried out on a Vapo Protect Eppendorf Thermal Cycler (Eppendorf, São Paulo, Brazil) following the amplification program with a preheating step of 94 °C for 2 min, 36 cycles of 94 °C for 1 min, 58 °C for 1 min, and 72 °C for 1 min; in the end, the extension step was at 72 °C for 5 min. All the PCR products were cleaned using 0.75 U of both enzyme EXO (Exonuclease I, Affimetrix, São Paulo, Brazil) and SAP (Shrimp Alkaline Phosphatase, Affimetrix, São Paulo, Brazil) in the proportion of 15 μL of PCR to 3 μL of the enzymes (diluted in 0.05 mol/L Tris, pH 8.0). Each reaction was incubated at 37 °C for 45 min to degrade the remaining primers and nucleotides, followed by one step at 80 °C for 20 min to inactivate the ExoSAP. Sequencing was performed by Macrogen Inc.

(South Korea), using the same primers as in the PCR amplifications. Sequences were edited and aligned using the program Sequencher 4.8 (Gene Codes Corporation, http://www.genecodes.com), using the default settings. In addition, the ReAligner (Anson & Myers, 1997) option was used to optimize gap placement. Gaps longer than three sites in the alignments were coded as insertions/deletions (indel), and different length indels were coded as different evolutionary events, following previous methodologies (e.g., Garcia et al., 2011; Zelener et al., 2016). We did not use indels that were bordered by mononucleotide repeats (e.g., polyA) as a source of information in subsequent statistical analyses to avoid effects that can arise from experimental errors or evolutionary lability associated with this type of indel (Mast et al., 2001).

2.4 Data analyses

For the microsatellite data, the populations with small sample sizes ($n < 9$; populations MDP, CON, SOO, PRD, FR2, CAM, and SMA) were included only in analyses that did not require an *a priori* identification of populations (as in Structure—see below). Initially, we estimated the null allele frequencies for each marker with the program Micro-Checker, version 2.2.3 (Van Oosterhout et al., 2004). Further, we used the software FSTAT, version 2.9.3.2 (Goudet, 2002) to calculate the statistical significance of deviation from the Hardy–Weinberg equilibrium (HWE) and linkage disequilibrium between loci in all populations. In order to describe the populations, we ran the GDA software (Lewis & Zaykin, 2002) and presented, for each population, the number of specimens (*n*), number of alleles per locus (*A/locus*), number of private alleles (A_{PRIV}), number of private alleles per specimens (A_{PRIV}/n), expected heterozygosity (H_E), observed heterozygosity (H_O), and inbreeding coefficient (F_{IS}). Concerning the diversity among populations, we estimated two indexes: F_{ST} (Weir & Cockerham, 1984) and R_{ST} (Slatkin, 1995; Goodman, 1997). The FSTAT software (Goudet, 2002) estimated both F_{ST} and R_{ST} over all samples. To test the significance of each estimate, we used 1000 permutations, with 99% confidence intervals. The F_{ST} index assumes the infinite alleles model, while the R_{ST} is based on allele size (stepwise mutation model, SMM). Estimates of R_{ST} may be useful when mutations contribute substantially to allelic differences among populations, resulting in greater insights into the patterns of relationships among populations than provided by F_{ST} (Holsinger & Weir, 2009). We also computed the pairwise F_{ST} of populations using ARLEQUIN (Excoffier et al., 2005). The *P*-value of the test is the proportion of permutations leading to an F_{ST} value larger or equal to the observed one (Manual of ARLEQUIN), we used 1000 permutations, with 95% confidence intervals. In Arlequin, we selected "Slantkin's distance" and instead of "Number of different alleles (F_{ST})" we activated the option "Sum of squared size difference (R_{ST})," which allowed us to use more information for each locus. In order to test whether gene flow or ancestral polymorphisms is the most important evolutionary force, we performed a Mantel test (Mantel, 1967) using the R package "*ade4*" (Jombart, 2008). If gene flow is an important evolutionary force, then the genetic differentiation of close population pairs should be lower than for those population pairs at larger geographic distances (Muir & Schloetterer, 2005). Thus, the R_{ST} would be correlated to the geographic distance between localities.

For the next genetic structure analysis, we included all 21 populations. The Bayesian clustering approach of software Structure version 2.3.4 (Pritchard et al., 2000; Hubisz et al., 2009) inferred the number of genetic groups of *C. fissilis* using the Monte Carlo Markov Chain (MCMC) approach. We set runs with a burn-in period of 250 000 steps followed by 750 000 steps, with 20 independent replications. The structure assumes a model in which there are *K* genetic groups, each of which is characterized by a set of allele frequencies at each locus. Individuals in the sample are assigned (probabilistically) to one or more genetic groups, if their genotypes indicate that they are an admixture (Pritchard et al., 2010). As Evanno et al. (2005) suggested, we set the *K* from 1 to 24, which is from 1 to the number of sampling sites (21) plus 3. To find the best *K*, we used the ΔK method (Evanno et al., 2005), as implemented in Structure Harvester (Earl & VonHoldt, 2011). The software CLUMPP (Jakobsson & Rosenberg, 2007) permuted the clusters output by independent runs of STRUCTURE and matched up the data of the 20 iterations into one: the best *K*. Later, we graphically displayed the results using the software DISTRUCT (Rosenberg, 2004). For each population, we summed the membership coefficients for all samples to obtain a diagram depicting the relative contribution of each lineage to the contemporary gene pool of that population.

In order to assess the diversity of the sequences obtained, the program DnaSP 5:10 (Librado & Rozas, 2009) determined the haplotypes in the data set. Gene genealogies based on the coalescent theory were inferred using a Median Joining haplotype network (Bandelt et al., 1999) as implemented in NETWORK 4.5.1.6 (www.fluxus-technology.com). Changes in the effective population size through time were inferred using a Bayesian Skyline approach (Ho & Shapiro, 2011) as implemented in BEAST v.2.4.4 (Drummond et al., 2012) using the cpDNA data. The analysis was run for 100 generations (to ensure sufficient sampling [ESS > 200]) using the HKY nucleotide substitution model and a strict molecular clock (5E-9 s/s/y). The first 10% of samples were discarded as burn-in prior to the Skyline reconstruction in Tracer (v.1.7).

3 Results

3.1 Habitat suitability modeling

Climate-based distribution models of *Cedrela fissilis*, built with current conditions, exhibited the best distance threshold of 860 km (AUC = 0.808). The models indicated the presence of fragmented highly suitable areas in the south of Brazil, as well as throughout the Atlantic coast. Habitat suitability varied substantially over the past 140 000 years (Fig. 2). High suitability during the LIG was predicted in a large area in southern Brazil (Fig. 2A, area 1) and in two smaller areas in the Paraná (Fig. 2A, area 2) and Amazon basin (Fig. 2A, area 3). Lower suitability was found in the Northeast during the LIG (Fig. 2A). During the LGM, the highest suitability shifted north and westward relative to the LIG projection (Fig. 2B). Also, high suitability on the then-exposed continental shelf was observed, especially at the Abrolhos Bank and the coast of the northeast (Fig. 2B). At the MidHol, similar to the present (Figs. 2C, 2D, respectively), high suitability regions were scattered south and eastward in Brazil, and also a small area in the north-

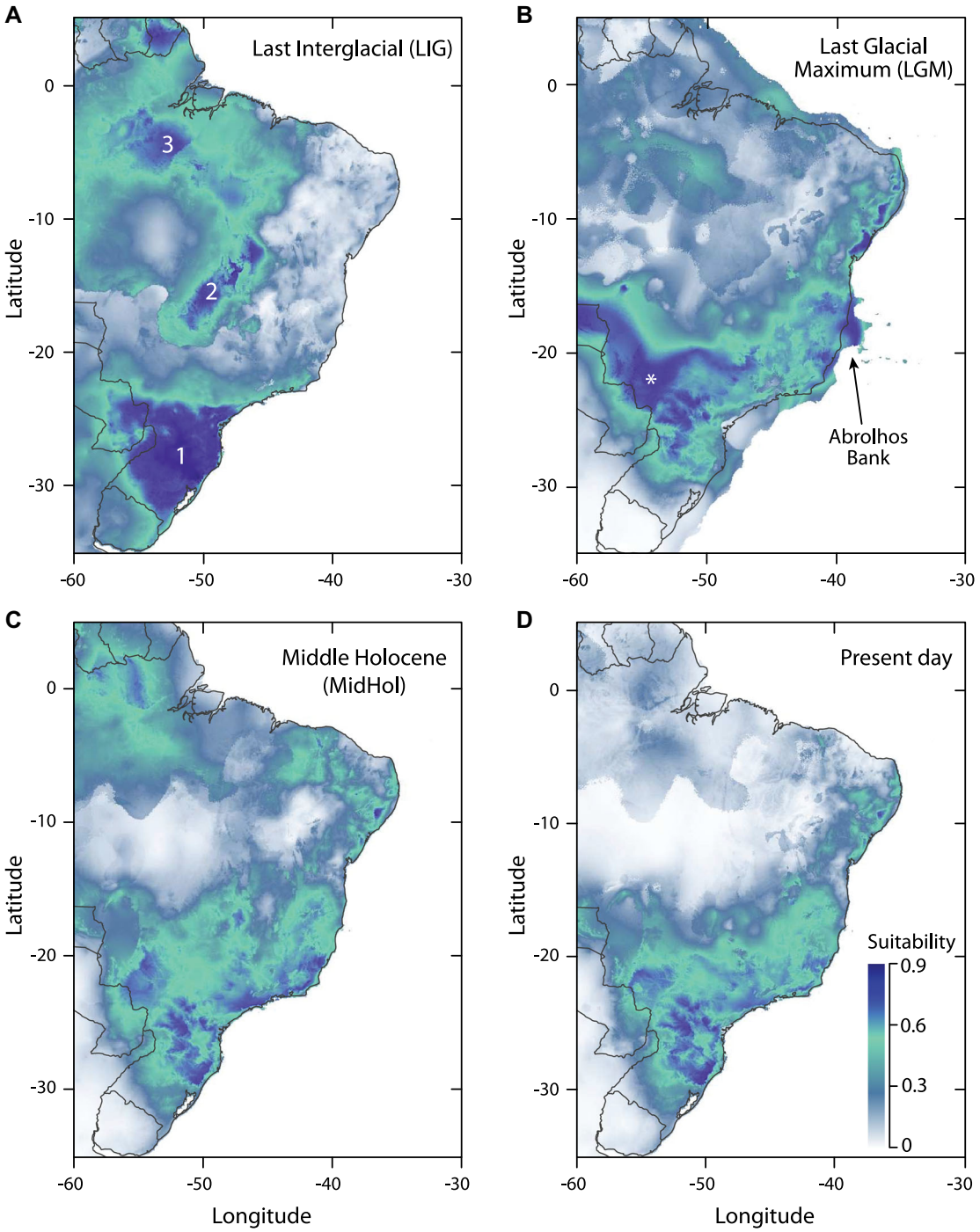


Fig. 2. Habitat suitability of *Cedrela fissilis* populations through time in eastern South America. Habitat suitability was projected onto **A,** the last interglacial (LIG, 140 000 to 120 000 y B.P.), **B,** the Last Glacial Maximum (LGM, 28 000 to 24 000 y B.P.), including the then exposed continental shelf, **C,** the Middle Holocene (MidHol, 6000 y B.P.), and **D,** the present. Numbers in **A** indicate regions of high suitability during the LIG; the asterisk in **B** shows areas with high suitability during the LGM. All plots use the same suitability scale shown in **D**.

east. These four time periods exhibited increased fragmentation through time toward the present day. For every cutoff (0.4, 0.5, 0.6, 0.7, and 0.8), the habitat fragmentation was higher in the present, followed by MidHol, LGM, and the LIG (Fig. 3).

3.2 Genetic diversity and structure

We identified 283 alleles across the 11 microsatellite loci; the number of alleles per locus ranged from 18 (Ced54) to 33 (Ced44). None of the 11 loci exhibited high null allele frequency (Table 2). Also, the 11 loci were at the Hardy-Weinberg

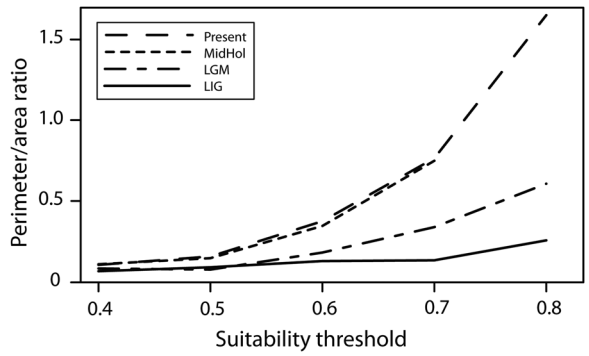


Fig. 3. Range fragmentation calculated as the perimeter/area ratio for each time (present, MidHol, Last Glacial Maximum [LGM], and last interglacial [LIG]) under different suitability thresholds (0.4 to 0.8).

equilibrium and linkage equilibrium. Fourteen populations (with population size ≥9) exhibited 61 private alleles (A_{priv}), ranging from 0 (SER) to 9 (PSO). When we divided A_{priv} by the number of samples, we picked up the A_{priv} regardless of the different population sizes; the highest A_{priv}/n occurred in the populations UBE ($A_{priv}/n = 0.37$) and PSO ($A_{priv}/n = 0.36$). The mean expected heterozygosity was $H_E = 0.83$, with values ranging from $H_E = 0.7$ (SER) to $H_E = 0.88$ (TBA), while the observed heterozygosity was $H_O = 0.72$, with values ranging from $H_O = 0.61$ (SER) to $H_O = 0.79$ (TBA). The H_E was slightly higher than H_O, indicating some degree of inbreeding in all populations. The mean inbreeding coefficient was $F = 0.14$, with values ranging from $F = 0.11$ (CAP) to $F = 0.24$ (PSB) (Table 1). We detected a significant, but low F_{ST} over all 14 populations ($F_{ST} = 0.058$, $P < 0.01$). Similarly, the R_{ST} was significant and low ($R_{ST} = 0.0826$, $P < 0.01$). Since the R_{ST} value was higher than F_{ST}, the observed differentiation among the populations received a strong contribution of the SMM. Thus, the pairwise genetic diversity was calculated with the matrix of Slatkin's linearized F_{ST}. For the pairwise R_{ST} (Table 3), we obtained 65 significant values ($P < 0.05$) out of 91 pairwise values. The genetically closest populations were UBE x ITA ($R_{ST} = 0.019$), and the genetically farthest populations were SER x VNI ($R_{ST} = 0.225$). The population SER exhibited higher pairwise values when compared to other populations. The Mantel test revealed a significant correlation between R_{ST} and geographic distances ($P < 0.001$), suggesting that gene flow is the main driver of the observed patterns.

The genetic structure of the 21 populations (also including populations $n < 9$) was placed along the BAF (Fig. 4A) and assigned to five genetic groups ($K = 5$, Figs. 4B, 4C). Populations with a majority of genetic group 1 (PSO, PNI, CAM, and BLU) were mainly distributed along the coast of the southeast ("Serra do Mar" in dark blue, Fig. 4A) with one exception (CON), which can be found further north in close proximity to populations from other genetic groups (SOO and PRD). Populations CAM, BLU, and CON belong to low elevations, while the populations PSO and PNI are from highlands. Populations for which the majority genetic group is group 2 ("Central-West" in light blue, Fig. 4A) are widely spread in central Brazil, occurring both in lowlands (ITA, FR2, UBE, DIA, and PRD) and highlands (PSB and PEU). Three populations from the lowland (PLO, TBA, and SMA) exhibited major assignment to genetic group 3 ("South" in yellow, Fig. 4A). The highland population PNI was also associated with group 3. Genetic group 4 ("Serra do Caparaó" in green, Fig. 4A) occurred especially in highland populations, with a high proportion in CAP and VNI, and also in the populations PRD and MDP. The latter population was the one with the highest level of admixture. Finally, the genetic group 5, ("Northeast" in turquoise, Fig. 4A), occurred in three lowland populations (JAN, SER, and SOO).

3.3 Phylogeographic patterns

The alignment of 1370 bp revealed the presence of 20 polymorphic sites, and indels or substitutions in 148 individuals. We observed 19 substitutions, 5 transitions, and 15 transversions. The remaining polymorphic sites were represented by an indel of seven base pairs. The analysis of 148 specimens of *Cedrela fissilis* revealed 16 haplotypes (Fig. S2).

Table 3 Matrix of Slatkin's linearized pairwise F_{ST} for 14 populations of *Cedrela fissilis*

	SER	JAN	UBE	DIA	PEU	VNI	CAP	PSB	ITA	PSO	PNI	TBA	PLO	BLU
SER	–													
JAN	0.049	–												
UBE	0.184	ns	–											
DIA	0.168	ns	ns	–										
PEU	0.197	ns	0.025	0.041	–									
VNI	0.225	ns	0.097	0.097	0.073	–								
CAP	0.175	ns	0.070	0.052	0.072	ns	–							
PSB	0.172	ns	0.036	0.065	0.043	0.103	0.072	–						
ITA	0.155	0.030	0.019	0.036	0.058	0.079	0.040	0.030	–					
PSO	0.119	ns	ns	ns	ns	ns	ns	ns	ns	–				
PNI	0.178	ns	0.030	0.025	0.047	0.070	0.039	0.038	0.024	ns	–			
TBA	0.156	ns	0.037	0.022	0.050	0.077	0.043	0.040	ns	ns	0.021	–		
PLO	0.154	0.021	0.026	0.023	0.042	0.084	0.036	0.044	0.024	ns	ns	ns	–	
BLU	0.172	ns	0.095	0.081	0.086	0.097	0.068	0.075	0.066	ns	0.054	0.064	0.042	–

Note: All pairwise values shown are significant ($P > 0.05$), while "ns" indicates non-significant pairwise F_{ST} values.

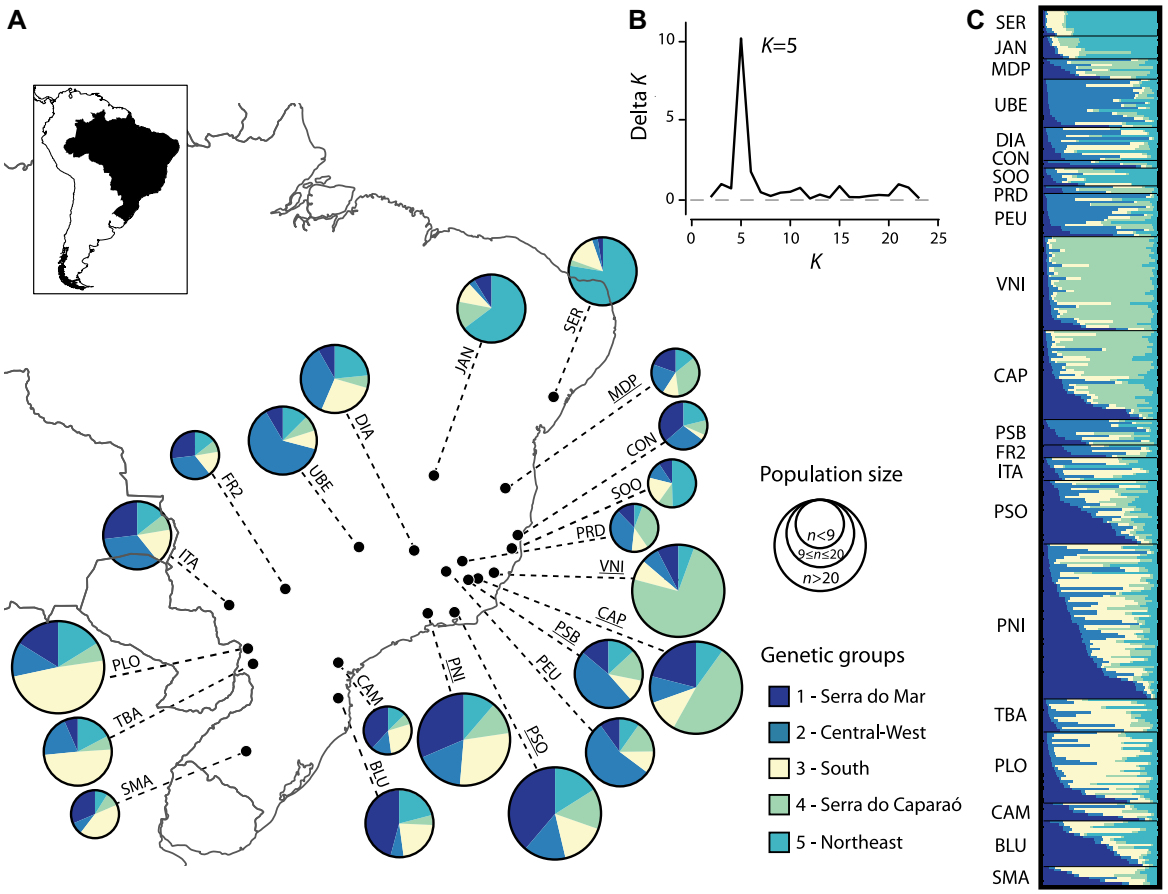


Fig. 4. Cluster analysis and geographic distribution of the five genetic groups of *Cedrela fissilis*. **A,** Geographic distribution and lineage assignments of all populations. Pie charts represent the mean of each membership coefficient for all samples from that population. **B,** The ΔK statistic, based on the second order rate of change of the likelihood function, identified $K = 5$ as the best-fit number of genetic groups. **C,** Plot of the cluster analysis in STRUCTURE. Each horizontal bar represents an individual, colors indicate a membership coefficient that represents the fraction of the genome that has ancestry in the respective genetic group (refer to Table S1 for population codes).

Every haplotype was placed on a map (Fig. 5A), and the seven genealogical lineages (hereafter haplogroups) were depicted in a haplotype network (Fig. 5B). The central haplogroup (H1, in blue) was the most frequent. This haplogroup was represented by 66 specimens from 22 populations widely scattered in the Atlantic range. Haplogroups H4 (yellow) and H2, H3, and H6 (orange) exhibited an overlapping distribution in the south-west of Brazil, with the exception of population SOO, which occurred at the east coast. Haplogroups H7 and H14 (in lilac) and H5 (red) showed geographic overlap in the north-east of Brazil. The red haplogroup was connected to the central one (blue) by haplotypes from population VNI (H16). The lilac haplogroup were connected to the central one by haplotypes from population PSB (H13). The green haplogroup (H8) was the farthest from the central haplogroup, separated by six mutational steps. This haplogroup showed evidence for a connection between the western and the eastern populations through the north-east. Five populations were very close geographically (in the western area), although each one belonged to a different haplogroup (CEC, FR2, OUR, CED, and SRP). Similar to the genetic structure of the populations, the haplogroups were not associated with elevation. The population demographic analysis indicated little changes of the effective population size (Bayesian Skyline plot, Fig. S3). This result corroborates findings of Mangaravite et al. (2016), who tested for heterozygosity excess in microsatellite data of *C. fisslis* and found no significant heterozygosity excess (which would be indicative of a genetic bottleneck) in any of the populations.

4 Discussion

In this study, we used species distribution modeling and two molecular markers (microsatellites and cpDNA) to assess the late-Quaternary evolutionary dynamics of the tree species *Cedrela fissilis* (Meliaceae) in the BAF and beyond. Our results provide support for both the moist forest as well as the DRH, suggesting that most likely a mixture of these processes have acted through space and time.

4.1 Moist forest hypothesis and connectivity during the LGM

The molecular data were largely congruent (between microsatellites and cpDNA), and minor differences may be

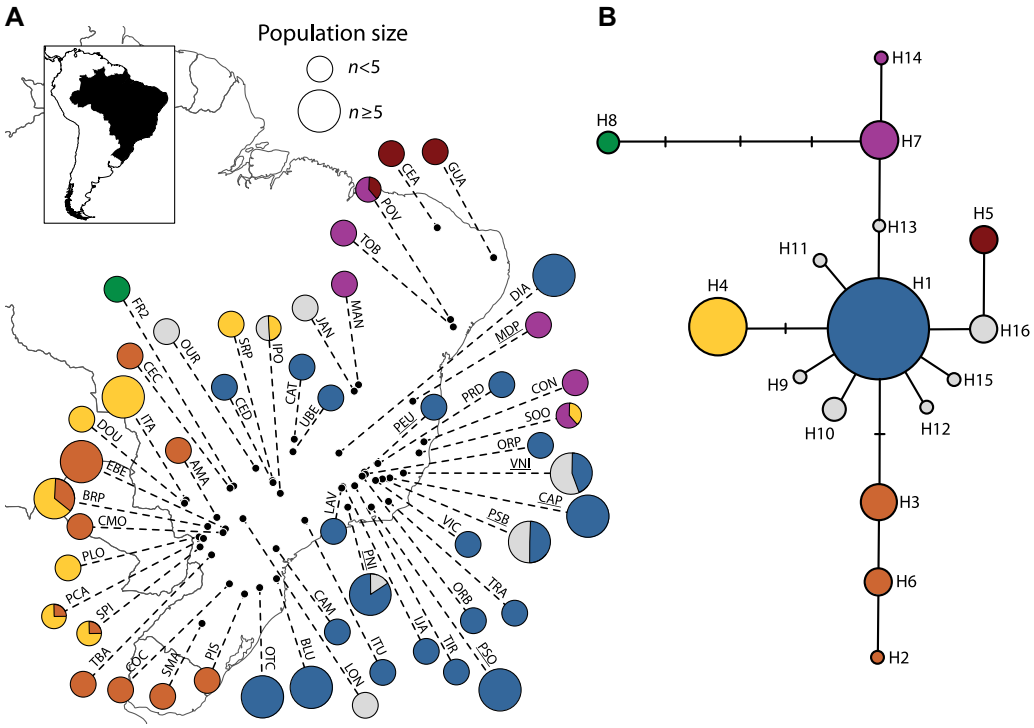


Fig. 5. Median-joining network and the geographic distribution of the 16 haplotypes of *Cedrela fissilis*. **A,** The geographic occurrences of the populations and their lineage assignment. Each pie chart represents one population, the colors depict the haplogroup which the population belongs to (see Table S1 for population codes). The size of the pie charts indicates population sizes. **B,** Median-joining network using *trnT-trnL* haplotypes. The network shows the relationships among different genealogical lineages of *C. fissilis*. Each circle represents one haplogroup (coded from H1 to H16), sizes are proportional to their relative frequencies. The number of mutational steps is indicated by small bars in case more than one step occurred.

due to higher mutation rates and high levels of polymorphism in the microsatellites (Schlötterer, 2000; Zane et al., 2002). Most of the populations of *C. fissilis* from the BAF exhibited a diffuse genetic structure, which could be the consequence of a range expansion and higher connectivity in the past, as suggested by the MFH (Ramírez-Barahona & Eguiarte, 2013). Some populations in the Atlantic coast close to the Abrolhos Bank (CON, SOO, and PRD) were highly admixed and seem to be a relic of an expansion onto the continental shelf during the LGM. Indeed, our predictions for the LGM show less fragmentation relative to the present, indicating a higher connectivity and gene flow, which has also been shown for marsupials (Leite et al., 2016). A low spatial genetic structure due to past connectivity was further reported in populations of the shrub *Myrtus nivellei* (Myrtaceae) in mountains in the Sahara Desert (Migliore et al., 2013) and in the montane salamander *Pseudoeurycea leprosa* in the Trans-Mexican Volcanic Belt (Velo-Antón et al., 2013). In the BAF, the weak genetic structure is not exclusive to *C. fissilis*. A similarly weak genetic structure was reported in birds and explained by the occurrence of bottleneck events (Batalha-Filho et al., 2012; Cabanne et al., 2013). However, for *C. fissilis*, bottlenecks are unlikely to have occurred given the homozygote excess observed here and in Mangaravite et al. (2016). Moreover, *C. fissilis* exhibits high variation within populations, even higher than the variation among the ranges of two distinct genealogical lineages (AMOVA analysis, Mangaravite et al., 2016). The diffuse genetic structure of *C. fissilis* populations is reflected in low pairwise F_{ST} values (with many values <0.05). Even though STRUCTURE correctly infers the genetic assignment when genetic differentiation among groups is low, only levels of genetic differentiation higher than 0.05 attain an accuracy rate of over 97% (Latch et al., 2006). This may explain the fact that populations VNI and SER (both with higher F_{ST} values) were the two populations with the least admixture in our STRUCTURE analysis.

The BAF biome harbors such a complex topography (Ab'Saber, 2005) that some studies reported, in contrast to our findings, the presence of populations with deep genetic structure (e.g., in toads; Thomé et al., 2010). In our study, some populations of *Cedrela fissilis* exhibited only little admixture (SER, JAN, UBE, PEU, CAP, and PSB), thus being genetically more structured than those mentioned above. Except for three populations (SER, JAN, and UBE), this strong genetic structure was found in highland populations, suggesting isolation by elevation, as found in a dominant tree, *Castanopsis eyrei* (Fagaceae), in the Nanling Mountains, China (Shi et al., 2011). However, in contrast to the populations of the *C. eyrei*, where gene flow among populations of similar elevations exceeded gene flow along an elevational gradient on individual mountains (Shi et al., 2011), highland populations of *C. fissilis* belonged to different genetic groups even in geographic proximity (e.g., PSB and

CAP). This distinct genetic structure observed in *C. fissilis* could be the result of three processes: (i) differentiation by genetic drift associated with upslope migration (with little to no evidence of present-day connection), (ii) long-distance dispersal onto the highlands from distinct source areas, or (iii) recolonization from nearby refugia. While some of these processes may have acted together, our data suggest that dispersal from different sources is most likely.

Dispersal ability is a key factor that influences gene flow (Freeland, 2005), and the level of admixture among populations of *C. fissilis* reflects gene flow likely by dispersal across the entire Atlantic range. Indeed, long-distance dispersal has been an important process that shaped not only the current distribution of *C. fissilis* (Garcia et al., 2011; Mangaravite et al., 2016), but the entire genus from deep time to the present (Muellner et al., 2010; Koecke et al., 2013). The low habitat suitability in the north-east of the Brazilian Atlantic coast during the LIG together with the strong genetic structure (genetic group 5 and haplotypes H5, H7, and H14) and high genetic divergence (see F_{ST} values of SER population) of the north-eastern populations suggest that long-distance dispersal to this region might have occurred following the late-Quaternary climatic fluctuations. Similar patterns of low admixture in the north-eastern area are known in frog species (Carnaval et al., 2009), birds (D'Horta et al., 2011; Maldonado-Coelho, 2012), spiders (Peres et al., 2017), and in wasp populations (Menezes et al., 2017). D'Horta et al. (2011) and Menezes et al. (2017) explained these patterns by a recent bottleneck effect, but our data suggest that the north-eastern populations harbor a combination of lineages that probably arrived during or after the LGM through different dispersal routes: one from inland (Amazonia), and another one from the coastal south-east. These two geographical routes were referred to as the "Peri-Amazonian" and the "Parana Atlantic" vegetation gradient, respectively, based on the analysis of the spatial distribution of 32 common tree species in South America (Spichiger et al., 2004). The phylogeographic connection between the FR2 population and the northeastern populations could constitute a relic of such a "Peri-Amazonian" dispersal. Indeed, FR2 and populations in the center of Brazil exhibit a high admixture pattern from either the Atlantic or Chiquitano range (Mangaravite et al., 2016; Diaz-Soto et al., 2018; Huamán-Mera, unpublished data). The "Parana Atlantic" route may have a high impact on the genetic diversity found in the northern *C. fissilis* populations, because the network analysis indicated two independent connections between the north-eastern and the Atlantic coast, suggesting independent dispersals. Moreover, the SER population (Fig. 4) and TOB and POV populations (Fig. 5) belong to the Atlantic range (rather than the Chiquitano range; Mangaravite et al., 2016). Finally, SER is the only population with no private alleles, which suggests that this population might not have been isolated long enough for its divergence. Others have argued that northern populations persisted in a refugium that allowed for their diversification, such as the "Pernambuco refugium" in frogs (Carnaval et al., 2009) or the "Caatinga" ancient refugium observed in palms (Souza et al., 2018). In contrast, we argue that in *C. fissilis* long-distance dispersal is more important for the genetic structure of the north-east region than a local refugium and its distinctiveness is likely due to a unique combination of alleles that exist at the intersection of two different dispersal routes.

4.2 Dry refugia hypothesis and the refugia concept

The ecotonal region of the BAF and the Cerrado in the Paraná basin is another highly diverse area for *Cedrela fissilis* (Figs. 4, 5) that might be the result of long-distance dispersal. This appears to be another intersection between the Central-West and South of Brazil due to the likely expansion during the LGM, which resulted in the advance of dry vegetation restricted to ecotonal conditions (Arruda et al., 2017). At that time, the Paraná basin was a humid region (Spichiger et al., 2004) and was suggested as having acted as a refugium due to climate stability (Carnaval & Moritz, 2008; Carnaval et al., 2009), leading to higher genetic diversity within and among populations compared to less stable areas (Carnaval et al., 2009). It should be noted that the term "refugium" usually refers to contractions of the geographic range in conjunction with reductions in abundance (Bennett & Provan, 2008; Stewart et al., 2010; Keppel et al., 2012). This reduction results in a loss of genetic diversity and a marked genetic structure as suggested by the DRH (Ramírez-Barahona & Eguiarte, 2013). In this sense, we would not apply the term refugium to the Paraná basin area, while not excluding the stability attribute. Gallery forests in the Paraná basin might have acted as a buffer and sustained forest-adapted lineages in dry regions (Fine & Lohmann, 2018), promoting the survival of drought-tolerant and generalist species, such as *C. fissilis* (Spichiger et al., 2004). However, instead of contraction, we argue that these populations experienced increased connectivity allowing an admixture genetic structure during the LGM. This does not reject the drier and cooler climate reported for the Southeast based on palynological data (Behling, 2002), as *C. fissilis* shifted its distribution toward central Brazil, and returning southward after the LGM. This is further corroborated by three additional findings: (i) high levels of admixture between the two genealogical lineages (Mangaravite et al., 2016), (ii) the presence of a new lineage in another ecotone, also between the Cerrado and the BAF (Diaz-Soto et al., 2018), and (iii) the discovery of a new species of *Cedrela* from the center of Brazil (Huamán-Mera et al., unpublished data). Additional sampling in the center of Brazil is required to increase the genetic structure resolution and to obtain a thorough history of the Paraná basin and its importance for the diversity in the BAF.

4.3 Conservation and future perspectives

Global warming impacts animal and plant populations, and will continue to do so in the future (Root et al., 2003). One potential future impact on *Cedrela fissilis* is increased fragmentation of suitable habitats. This fragmentation may lead to a substantial loss of genetic diversity, and put populations at the risk of extinction (Bálint et al., 2011), especially those occurring in highlands (La Sorte & Jetz, 2010; McCain & Colwell, 2011). *Cedrela fissilis* is classified as "vulnerable" in the Red List of the International Union for Conservation of Nature (IUCN), and its populations are declining (Barstow, 2018). Both these facts make *C. fissilis* an important focal species for studying the impact of climate change on tropical trees. Modeling the future distribution for *C. fissilis* will help to better forecast the climatic impact on this species, and hopefully help guide conservation measures.

Acknowledgements

The authors thank three anonymous reviewers for constructive comments on an earlier version of this manuscript. E.M. is grateful to CAPES (Coordenação de Aperfeiçoamento de Pessoal de Nível Superior) and CNPq (Conselho Nacional de Desenvolvimento Científico e Tecnológico) for providing a student fellowship in Brazil, and E.M. is also grateful to CAPES for providing an international student fellowship, supported by the program PDSE (Programa de Doutorado Sanduíche no Exterior), to visit the Senckenberg Biodiversity and Climate Research Centre (SBiK-F), Frankfurt (J.S.) and Leipzig University (A.N.M.-R.). L.O.O. received a fellowship from CNPq (PQ 304153/2012-5) and grants from FAPEMIG (Fundação de Amparo à Pesquisa do Estado de Minas Gerais) (PPM-00561-15, 18 BPD-00282-10) and CNPq (562249/2010-9). A.N.M-R. and J.S. were supported by the "LOEWE—Landes-Offensive zur Entwicklung Wissenschaftlich-oekonomischer Exzellenz" of Hesse's Ministry of Higher Education, Research, and the Arts. Additional support was provided by the German Centre for Integrative Biodiversity Research (iDiv) Halle-Jena-Leipzig funded by the German Research Foundation (DFG—FZT 118) to J.S.

References

Ab'Saber AN. 2005. *Os domínios de natureza no Brasil: Potencialidades paisagísticas*. São Paulo: Ateliê Editorial.

Almeida FFM, Carneiro CDR. 1998. Origem e evolução da serra do mar. *Revista Brasileira de Geociências* 28: 135–150.

Amaral FR, Albers PK, Edwards SV, Miyaki CY. 2013. Multilocus tests of Pleistocene refugia and ancient divergence in a pair of Atlantic Forest antbirds (*Myrmeciza*). *Molecular Ecology* 22: 3996–4013.

Amaro RC, Rodrigues MT, Yonenaga-Yassuda Y, Carnaval AC. 2012. Demographic processes in the montane Atlantic rainforest: Molecular and cytogenetic evidence from the endemic frog *Proceratophrys boiei*. *Molecular Phylogenetics and Evolution* 62: 880–888.

Anson EL, Myers EW. 1997. ReAligner: A program for refining DNA sequence multi-alignments. *Journal of Computational Biology* 4: 369–383.

Arruda DM, Fernandes-Filho EI, Solar RRC, Schaefer CEGR. 2017. Combining climatic and soil properties better predicts covers of Brazilian biomes. *The Science of Nature* 104: 32.

Bálint M, Domisch S, Engelhardt CHM, Haase P, Lehrian S, Sauer J, Theissinger K, Pauls SU, Nowak C. 2011. Cryptic biodiversity loss linked to global climate change. *Nature Climate Change* 1: 313–318.

Bandelt HJ, Forster P, Rohl A. 1999. Median-joining networks for inferring intraspecific phylogenies. *Molecular Biology and Evolution* 16: 37–48.

Barstow M. 2018. *Cedrela fissilis.* The IUCN Red List of Threatened Species 2018: e.T33928A68080477 [online]. Available from https://doi.org/10.2305/IUCN.UK.2018-1.RLTS.T33928A68080477.en [accessed 27 April 2019].

Batalha-Filho H, Cabanne GS, Miyaki CY. 2012. Phylogeography of an Atlantic forest passerine reveals demographic stability through the last glacial maximum. *Molecular Phylogenetics and Evolution* 65: 892–902.

Behling H. 2002. South and southeast Brazilian grasslands during Late Quaternary times: A synthesis. *Palaeogeography, Palaeoclimatology, Palaeoecology* 177: 19–27.

Bennett K, Provan J. 2008. What do we mean by 'refugia'? *Quaternary Science Reviews* 27: 2449–2455.

Bertoncello R, Yamamoto K, Meireles LD, Shepherd GJ. 2011. A phytogeographic analysis of cloud forests and other forest subtypes amidst the Atlantic Forests in south and southeast Brazil. *Biodiversity and Conservation* 20: 3413–3433.

Cabanne GS, Sari EHR, Meyer D, Santos FR, Miyaki CY. 2013. Matrilineal evidence for demographic expansion, low diversity and lack of phylogeographic structure in the Atlantic Forest endemic Greenish Schiffornis *Schiffornis virescens* (Aves: Tityridae). *Journal of Ornithology* 154: 371–384.

Carnaval AC, Hickerson MJ, Haddad CFB, Rodrigues MT, Moritz C. 2009. Stability predicts genetic diversity in the Brazilian Atlantic Forest hotspot. *Science* 323: 785–789.

Carnaval AC, Moritz C. 2008. Historical climate modelling predicts patterns of current biodiversity in the Brazilian Atlantic Forest. *Journal of Biogeography* 35: 1187–1201.

Carvalho PER. 1994. *Espécies florestais brasileiras: Recomendações silviculturais, potencialidades e uso da madeira*. Brasilia, Brazil: EMBRAPA-SPI.

Colinvaux PA, De Oliveira PE, Bush MB. 2000. Amazonian and neotropical plant communities on glacial time-scales: The failure of the aridity and refuge hypotheses. *Quaternary Science Reviews* 19: 141–169.

Conservation International. 2018. Hotspots [online]. Available from https://www.conservation.org/How/Pages/Hotspots.aspx [accessed 20 January 2019].

Cota-Sánchez JH, Remarchuk K, Ubayasena K. 2006. Ready-to-use DNA extracted with a CTAB method adapted for herbarium specimens and mucilaginous plant tissue. *Plant Molecular Biology Reporter* 24: 161–167.

Diaz-Soto JM, Huamán-Mera A, Oliveira LO. 2018. Population genetics of *Cedrela fissilis* (Meliaceae) from an ecotone in central Brazil. *Tree Genetics & Genomes* 14: 73.

D'Horta FM, Cabanne GS, Meyer D, Miyaki CY. 2011. The genetic effects of Late Quaternary climatic changes over a tropical latitudinal gradient: Diversification of an Atlantic Forest passerine. *Molecular Ecology* 20: 1923–1935.

Drummond A, Suchard M, Xie D, Rambaut A. 2012. Bayesian phylogenetics with BEAUti and the BEAST 1.7. *Molecular Biology and Evolution* 29: 1969–1973.

Earl DA, VonHoldt BM. 2011. STRUCTURE HARVESTER: A website and program for visualizing STRUCTURE output and implementing the Evanno method. *Conservation Genetics Resources* 4: 359–361.

Elsen PR, Tingley MW. 2015. Global mountain topography and the fate of montane species under climate change. *Nature Climate Change* 5: 772–776.

Evanno G, Regnaut S, Goudet J. 2005. Detecting the number of clusters of individuals using the software STRUCTURE: A simulation study. *Molecular Ecology* 14: 2611–2620.

Excoffier L, Laval G, Schneider S. 2005. Arlequin (version 3.0): An integrated software package for population genetics data analysis. *Evolutionary Bioinformatics* 1: 47–50.

Fine PVA, Lohmann LG. 2018. Importance of dispersal in the assembly of the Neotropical biota. *Proceedings of the National Academy of Sciences USA* 115: 5829–5831.

Freeland J. 2005. *Molecular ecology*. Chichester, UK: John Wiley & Sons.

Gandara FB. 2009. *Diversidade genética de populações de cedro (Cedrela ssilis Vell. (Meliaceae) no centro-sul do Brasil*. Ph.D. Thesis. São Paulo, Brazil: University of São Paulo.

Gandara FB, Tambarussi EV, Sebbenn AM, Ferraz EM, Moreno MA, Ciampi AY, Vianello RP, Grattapaglia D, Kageyama PY. 2014. Development and characterization of microsatellite loci for *Cedrela fissilis* Vell (Meliaceae), an endangered tropical tree species. *Silvae Genetica* 63: 240–243.

Garcia MG, Silva RS, Carniello MA, Veldman JW, Rossi AAB, de Oliveira LO. 2011. Molecular evidence of cryptic speciation, historical range expansion, and recent intraspecific hybridization in the Neotropical seasonal forest tree *Cedrela fissilis* (Meliaceae). *Molecular Phylogenetics and Evolution* 61: 639–649.

Gent PR, Danabasoglu G. 2011. Response to increasing southern hemisphere winds in CCSM4. *Journal of Climate* 24: 4992–4998.

Giorgetta MA, Jungclaus J, Reick CH, Legutke S, Bader J, Böttinger M, Brovkin V, Crueger T, Esch M, Fieg K. 2013. Climate and carbon cycle changes from 1850 to 2100 in MPI-ESM simulations for the Coupled Model Intercomparison Project phase 5. *Journal of Advances in Modeling Earth Systems* 5: 572–597.

Goodman SJ. 1997. Rst Calc: A collection of computer programs for calculating estimates of genetic differentiation from microsatellite data and determining their significance. *Molecular Ecology* 6: 881–885.

Goudet J. 2002. FSTAT: A program to estimate and test gene diversities and fixation indices. Available from http://www2.unil.ch/popgen/softwares/fstat.htm [accessed 01 June 2017].

Haffer J. 1969. Speciation in Amazonian Forest Birds. *Science* 165: 131–137.

Hammen TV, Hooghiemstra H. 2000. Neogene and Quaternary history of vegetation, climate, and plant diversity in Amazonia. *Quaternary Science Reviews* 19: 725–742.

Hanley JA, McNeil BJ. 1982. The meaning and use of the area under a receiver operating characteristic (ROC) curve. *Radiology* 143: 29–36.

Hernández G, Buonamici A, Walker K, Vendramin GG, Navarro C, Cavers S. 2008. Isolation and characterization of microsatellite markers for *Cedrela odorata* L. (Meliaceae), a high value neotropical tree. *Conservation Genetics* 9: 457–459.

Hewitt G. 2000. The genetic legacy of the Quaternary ice ages. *Nature* 405: 907–913.

Hijmans RJ, Cameron S, Parra J, Jones PG, Jarvis A, Richardson K. 2005. *WorldClim, version 1.3*. Berkeley: University of California.

Ho SY, Shapiro B. 2011. Skyline-plot methods for estimating demographic history from nucleotide sequences. *Molecular Ecology Resources* 11: 423–434.

Holsinger KE, Weir BS. 2009. Genetics in geographically structured populations: Defining, estimating and interpreting F(ST). *Nature Reviews Genetics* 10: 639–650.

Homburg K, Drees C, Gossner MM, Rakosy L, Vrezec A, Assmann T. 2013. Multiple glacial refugia of the low-dispersal ground beetle *Carabus irregularis:* Molecular data support predictions of species distribution models. *PLoS One* 8: e61185.

Hubisz MJ, Falush D, Stephens M, Pritchard JK. 2009. Inferring weak population structure with the assistance of sample group information. *Molecular Ecology Resources* 9: 1322–1332.

Hughes PD, Gibbard PL. 2015. A stratigraphical basis for the Last Glacial Maximum (LGM). *Quaternary International* 383: 174–185.

Iturbide M, Bedia J, Herrera S, del Hierro O, Pinto M, Gutiérrez JM. 2015. A framework for species distribution modelling with improved pseudo-absence generation. *Ecological Modelling* 312: 166–174.

Jakobsson M, Rosenberg NA. 2007. CLUMPP: A cluster matching and permutation program for dealing with label switching and multimodality in analysis of population structure. *Bioinformatics* 23: 1801–1806.

Jombart T. 2008. adegenet: A R package for the multivariate analysis of genetic markers. *Bioinformatics* 24: 1403–1405.

Keppel G, Van Niel KP, Wardell-Johnson GW, Yates CJ, Byrne M, Mucina L, Schut AGT, Hopper SD, Franklin SE. 2012. Refugia: Identifying and understanding safe havens for biodiversity under climate change. *Global Ecology and Biogeography* 21: 393–404.

Kier G, Kreft H, Lee TM, Jetz W, Ibisch PL, Nowicki C, Mutke J, Barthlott W. 2009. A global assessment of endemism and species richness across island and mainland regions. *Proceedings of the National Academy of Sciences USA* 106: 9322–9327.

Koecke AV, Muellner-Riehl AN, Cáceres O, Pennington TD. 2015. *Cedrela ngobe* (Meliaceae), a new species from Panama and Costa Rica. *Edinburgh Journal of Botany* 72: 225–233.

Koecke AV, Muellner-Riehl AN, Pennington TD, Schorr G, Schnitzler J. 2013. Niche evolution through time and across continents: The story of Neotropical *Cedrela* (Meliaceae). *American Journal of Botany* 100: 1800–1810.

La Sorte FA, Jetz W. 2010. Projected range contractions of montane biodiversity under global warming. *Proceedings of the Royal Society B: Biological Sciences* 277: 3401–3410.

Latch EK, Dharmarajan G, Glaubitz JC, Rhodes OE. 2006. Relative performance of Bayesian clustering software for inferring population substructure and individual assignment at low levels of population differentiation. *Conservation Genetics* 7: 295–302.

Leite YLR, Costa LP, Loss AC, Rocha RG, Batalha-Filho H, Bastos AC, Quaresma VS, Fagundes V, Paresque R, Passamani M, Pardini R. 2016. Neotropical forest expansion during the last glacial period challenges refuge hypothesis. *Proceedings of the National Academy of Sciences USA* 113: 1–6.

Lewis PO, Zaykin D. 2002. Genetic data analysis: Computer program for the analysis of allelic data. Available from http://phylogeny.uconn.edu/software/ [accessed 01 June 2017].

Librado P, Rozas J. 2009. DnaSP v5: A software for comprehensive analysis of DNA polymorphism data. *Bioinformatics* 25: 1451–1452.

Maldonado-Coelho M. 2012. Climatic oscillations shape the phylogeographical structure of Atlantic Forest fire-eye antbirds (Aves: Thamnophilidae). *Biological Journal of the Linnean Society* 105: 900–924.

Mangaravite E, Vinson CC, Rody HVS, Garcia MG, Carniello MA, Silva RS, Oliveira LO. 2016. Contemporary patterns of genetic diversity of *Cedrela fissilis* offer insight into the shaping of seasonal forests in eastern South America. *American Journal of Botany* 103: 307–316.

Mannion PD, Upchurch P, Benson RB, Goswami A. 2014. The latitudinal biodiversity gradient through deep time. *Trends in Ecology & Evolution* 29: 42–50.

Mantel N. 1967. The detection of disease clustering and a generalized regression approach. *Cancer Research* 27: 209–220.

Mast AR, Kelso S, Richards AJ, Lang DJ, Feller DMS, Conti E. 2001. Phylogenetic relationships in *Primula* L. and related genera (Primulaceae) based on noncoding chloroplast DNA. *International Journal of Plant Sciences* 162: 1381–1400.

Mateo RG, Croat TB, Felicísimo ÁM, Muñoz J. 2010. Profile or group discriminative techniques? Generating reliable species distribution models using pseudo-absences and target-group absences from natural history collections. *Diversity and Distributions* 16: 84–94.

McCain CM, Colwell RK. 2011. Assessing the threat to montane biodiversity from discordant shifts in temperature and precipitation in a changing climate. *Ecology Letters* 14: 1236–1245.

Meireles LD, Kinoshita LS, Shepherd GJ. 2014. Composição florística da vegetação altimontana do distrito de Monte Verde (Camanducaia, MG), Serra da Mantiqueira Meridional, Sudeste do Brasil. *Rodriguésia* 65: 831–859.

Meireles LD, Shepherd GJ. 2015. Structure and floristic similarities of upper montane forests in Serra Fina mountain range, south-eastern Brazil. *Acta Botanica Brasilica* 29: 58–72.

Menezes RST, Brady SG, Carvalho AF, Lama MADel, Costa MA. 2017. The roles of barriers, refugia, and chromosomal clines underlying diversification in Atlantic Forest social wasps. *Scientific Reports* 7: 1–16.

Migliore J, Baumel A, Juin M, Fady B, Roig A, Duong N, Médail F. 2013. Surviving in mountain climate refugia: New insights from the genetic diversity and structure of the relict shrub *Myrtus nivellei* (Myrtaceae) in the Sahara Desert. *PLoS One* 8: e73795.

Mix AC, Bard E, Schneider R. 2001. Environmental processes of the ice age: Land, oceans, glaciers (EPILOG). *Quaternary Science Reviews* 20: 627–657.

Muellner AN, Pennington TD, Chase MW. 2009. Molecular phylogenetics of Neotropical Cedreleae (mahogany family, Meliaceae) based on nuclear and plastid DNA sequences reveal multiple origins of *Cedrela odorata*. *Molecular Phylogenetics and Evolution* 52: 461–469.

Muellner AN, Pennington TD, Koecke AV, Renner SS. 2010. Biogeography of *Cedrela* (Meliaceae, Sapindales) in Central and South America. *American Journal of Botany* 97: 511–518.

Muellner-Riehl AN. 2019. Mountains as evolutionary arenas: Patterns, emerging approaches, paradigm shifts, and their implications for plant phylogeographic research in the Tibeto-Himalayan region. *Frontiers in Plant Science* 10, Article 195.

Muir G, Schloetterer C. 2005. Evidence for shared ancestral polymorphism rather than recurrent gene flow at microsatellite loci differentiating two hybridizing oaks (*Quercus* spp.). *Molecular Ecology* 14: 549–561.

Myers N, Mittermeier RA, Mittermeier CG, da Fonseca GAB, Kent J. 2000. Biodiversity hotspots for conservation priorities. *Nature* 403: 853–858.

Oliveira-Filho A, Fontes MA. 2000. Patterns of floristic differentiation among Atlantic Forests in southeastern Brazil and the influence of climate. *Biotropica* 32: 793–810.

Oliveira LO, Rossi AAB, Martins ER, Batista FRDC, Silva RS. 2010. Molecular phylogeography of *Carapichea ipecacuanha*, an amphi-tropical shrub that occurs in the understory of both semideciduous and evergreen forests. *Molecular Ecology* 19: 1410–1422.

Olson DM, Dinerstein E, Wikramanayake ED, Burgess ND, Powell GVN, Underwood EC, D'Amico JA, Itoua I, Strand HE, Morrison JC, Loucks CJ, Allnutt TF, Ricketts TH, Kura Y, Lamoreux JF, Wettengel WW, Heado P, Kassem KR, 2001. Terrestrial ecoregions of the world: A new map of live on earth. *Bioscience* 51: 933–937.

Otto-Bliesner BL, Marshall SJ, Overpeck JT, Miller GH. 2006. Simulating Arctic climate warmth and icefield retreat in the last interglaciation. *Science* 311: 1751–1753.

Pennington TD, Muellner AN. 2010. *A monograph of Cedrela (Meliaceae)*. Sherborne, UK: DH Books.

Pennington TD, Stules BT, Taylor DAH. 1981. Meliaceae. *Flora Neotropica* 28: 406–419.

Peres EA, Silva MJ, Solferini VN. 2017. Phylogeography of the spider *Araneus venatrix* (Araneidae) suggests past connections between Amazon and Atlantic rainforests. *Biological Journal of the Linnean Society* 121: 771–785.

Phillips SJ, Anderson RP, Schapire RE. 2006. Maximum entropy modeling of species geographic distributions. *Ecological Modelling* 190: 231–259.

Pompeu PV, Fontes MAL, Santos RM, Garcia PO, Batista TA, Carvalho WAC, Oliveira Filho AT. 2014. Floristic composition and structure of an upper montane cloud forest in the Serra da Mantiqueira Mountain Range of Brazil. *Acta Botanica Brasilica* 28: 456–464.

Pritchard JK, Stephens M, Donnelly P. 2000. Inference of population structure using multilocus genotype data. *Genetics* 155: 945–959.

Pritchard JK, Wen X, Falush D. 2010. Documentation for structure software: Version 2.3. Available from http://pritch.bsd.uchicago.edu [accessed 01 June 2017].

Ramírez-Barahona S, Eguiarte LE. 2013. The role of glacial cycles in promoting genetic diversity in the Neotropics: The case of cloud forests during the Last Glacial Maximum. *Ecology and Evolution* 3: 725–738.

Riahi M, Zarre S, Maassoumi AA, Attar F, Kazempour Osaloo S. 2010. An inexpensive and rapid method for extracting papilionoid genomic DNA from herbarium specimens. *Genetics and Molecular Research* 9: 1334–1342.

Ribeiro MC, Metzger JP, Martensen AC, Ponzoni FJ, Hirota MM. 2009. The Brazilian Atlantic Forest: How much is left, and how is the remaining forest distributed? Implications for conservation. *Biological Conservation* 142: 1141–1153.

Root TL, Price JT, Hall KR, Schneider SH. 2003. Fingerprints of global warming on wild animals and plants. *Nature* 421: 1–35.

Rosenberg NA. 2004. Distruct: A program for the graphical display of population structure. *Molecular Ecology Notes* 4: 137–138.

Rull V. 2008. Speciation timing and neotropical biodiversity: The Tertiary-Quaternary debate in the light of molecular phylogenetic evidence. *Molecular Ecology* 17: 2722–2729.

Schlötterer C. 2000. Evolutionary dynamics of microsatellite DNA. *Chromosoma* 109: 365–371.

Shi MM, Michalski SG, Chen XY, Durka W. 2011. Isolation by elevation: Genetic structure at neutral and putatively non-neutral loci in a dominant tree of subtropical forests, Castanopsis eyrei. *PLoS One* 6: e21302.

Silva SM, Moraes-Barros N, Ribas CC, Ferrand N, Morgante JS. 2012. Divide to conquer: A complex pattern of biodiversity depicted by vertebrate components in the Brazilian Atlantic Forest. *Biological Journal of the Linnean Society* 107: 39–55.

Slatkin M. 1995. A measure of population subdivision based on microsatellite allele frequencies. *Genetics* 139: 457–462.

Souza MCP, Moura F, Silva JV, Almeida C. 2018. Phylogeography of the palm *Syagrus coronata* (Martius) Beccari (Arecaceae): Distribution in the "Caatinga" and Atlantic forest domains. *Brazilian Journal of Botany* 41: 849–857.

Spichiger R, Calenge C, Bise B. 2004. Geographical zonation in the Neotropics of tree species characteristic of the Paraguay-Paraná Basin. *Journal of Biogeography* 31: 1489–1501.

Stewart JR, Lister AM, Barnes I, Dalén L. 2010. Refugia revisited: Individualistic responses of species in space and time. *Proceedings of the Royal Society B: Biological Sciences* 277: 661–671.

Tabarelli M, Pinto LP, Silva JMC, Hirota M, Bede L. 2005. Challenges and opportunities for biodiversity conservation in the Brazilian Atlantic Forest. *Conservation Biology* 19: 695–700.

Taberlet P, Gielly L, Pautou G, Bouvet J. 1991. Universal primers for amplification of three non-coding regions of chloroplast DNA. *Plant Molecular Biology* 17: 1105–1109.

Thomé MTC, Zamudio KR, Giovanelli JGR, Haddad CFB, Baldissera FA, Alexandrino J. 2010. Phylogeography of endemic toads and post-Pliocene persistence of the Brazilian Atlantic Forest. *Molecular Phylogenetics and Evolution* 55: 1018–1031.

VanDerWal J, Falconi L, Januchowski S, Shoo L, Storlie C, VanDerWal MJ. 2014. Package 'SDMTools'. Available from http://www.rforge.net/SDMTools/ [accessed 15 October 2016].

Van Oosterhout C, Hutchinson WF, Wills DPM, Shipley P. 2004. Micro-Checker: Software for identifying and correcting genotyping errors in microsatellite data. *Molecular Ecology Notes* 4: 535–538.

Velo-Antón G, Parra JL, Parra-Olea G, Zamudio KR. 2013. Tracking climate change in a dispersal-limited species: Reduced spatial and genetic connectivity in a montane salamander. *Molecular Ecology* 22: 3261–3278.

Watanabe S, Hajima T, Sudo K, Nagashima T, Takemura T, Okajima H, Nozawa T, Kawase H, Abe M, Yokohata T. 2011. MIROC-ESM 2010: Model description and basic results of CMIP5-20c3m experiments. *Geoscientific Model Development* 4: 845–872.

Weir BS, Cockerham CC. 1984. Estimating F-statistics for the analysis of population structure. *Evolution* 38: 1358–1370.

Zane L, Bargelloni L, Patarnello T. 2002. Strategies for microsatellite isolation: A review. *Molecular Ecology* 11: 1–16.

Zelener N, Tosto D, de Oliveira LO, Soldati MC, Inza MV, Fornes LF. 2016. Molecular evidence of hybrid zones of *Cedrela* (Meliaceae) in the Yungas of Northwestern Argentina. *Molecular Phylogenetics and Evolution* 102: 45–55.

Supplementary Material

The following supplementary material is available online for this article at http://onlinelibrary.wiley.com/doi/10.1111/jse.12545/suppinfo:

Table S1. Populations of *Cedrela fissilis* sampled for phylogeographic analyses (*n* = number of individuals).

Table S2. Pairwise Pearson correlation coefficients among all 19 bioclimatic variables. Labels and correlation coefficients of the seven selected predictor variables are in bold (see Table S3 for the full name of each variable).

Table S3. Percentage contribution and permutation importance in the Maxent models for all 19 variables (the subset of seven predictors are highlighted in bold).

Table S4. Percentage contribution and permutation importance for the retained subset of seven predictors in the final Maxent model.

Fig. S1. Digital elevation model of eastern South America with the locations of sampled populations of *Cedrela fissilis* (see Supporting Table S1 for population codes).

Fig. S2. *trnT-trnL* haplotypes. Out of 1370 sites, 20 were polymorphic in the two cpDNA fragments (fragment AB and fragment CD) of the 16 haplotypes (H1 to H16) from 148 specimens of *Cedrela fissilis*. Dots indicate similarity to haplotype 1, hyphens indicate gaps. Numbers on top indicate the nucleotide position with haplotype 1, acting as the reference sequence during alignment. The number (#) indicates the frequency of the haplotypes.

Fig. S3. Demographic history of *C. fissilis* estimated using Bayesian skyline plots from cpDNA data. The black line represents the mean estimate of the effective population size (*Ne*, log-scale) through time; the blue area indicates the upper and lower 95% highest posterior density (HPD) limits of *Ne*.